

## Evolution of SST and SSS in the Northern Bay of Bengal

Suryachandra A. Rao<sup>1</sup>, Subodh K. Saha<sup>1</sup>, Samir Pokhrel<sup>1</sup>,  
Damodaran Sundar<sup>2</sup>, Ashish R. Dhakate<sup>1</sup>, Somnath Mahapatra<sup>1</sup>,  
Sabeer Ali<sup>1</sup>, Hemantkumar S. Chaudhari<sup>1</sup>, P. Shreeram<sup>1</sup>, Suneel  
Vasimalla<sup>2</sup>, A. S. Srikanth<sup>3</sup>, R. R. V. Suresh<sup>3</sup>

Published Title: Modulation of SST, SSS over northern Bay of Bengal on ISO time scale

<sup>1</sup>Indian Institute of Tropical Meteorology, Pune, India

<sup>2</sup>National Institute of Oceanography, Goa, India

<sup>3</sup>Department of Meteorology & Oceanography, Andhra University,  
Visakhapatnam, India

### Corresponding author address :

A. Suryachandra Rao  
Indian Institute of Tropical Meteorology  
Pune 411008, India  
e-mail: surya@tropmet.res.in,  
Phone: +91 20 25904245  
Fax : +91 20 25893825

## Abstract

3 High resolution observations of atmospheric and oceanic variables are carried out at  
4 northern Bay of Bengal from 22<sup>nd</sup> July to 6<sup>th</sup> August 2009 on-board ORV Sagarkanya  
5 under the Continental Tropical Convergence Zone research/observational programme.  
6 Freshening of surface layer by more than 4 *psu* within 24 hours is observed, which  
7 is followed by warming in the surface layer temperature. The heat and salt budget  
8 analysis primarily indicates dominant role of advection processes on the evolution  
9 of temperature and salinity. The amount of rainfall received at observation site  
10 could not explain the observed freshening, thus an extensive analysis using wavelet  
11 coherence is done to find out the source of advected fresh water to the observed  
12 location. **It is found that surface salinity in the northern Bay of Bengal**  
13 **(at 15°N) varies coherently with the rainfall over Ganga-Brahmaputra**  
14 **catchment area on intraseasonal time scale and with lag of about 60**  
15 **days.** Based on above observations, this study hypothesize that the intraseasonal  
16 rainfall variation modulates the amount of river discharge, which in turn modulates  
17 the salinity over northern Bay of Bengal on intraseasonal time scale. Since surface  
18 warming always follows the surface freshening, the time delay between the rainfall  
19 over catchment area and freshening at northern Bay of Bengal may explain the  
20 post monsoon warming. Importance of atmosphere-ocean coupling in driving the  
21 dynamics of the **northern** bay of Bengal has been clearly brought out in this study.

## 22 1 Introduction

23 The northern Bay of Bengal (BoB) during summer monsoon (June-September) is  
24 generally characterized by high sea surface temperature (SST), shallow surface layer  
25 of low salinity and weak wind compared to the Arabian Sea (*Shenoi et al., 2002*;  
26 *Sprintall and Tomczak, 1992*; *McCreary et al., 1993*; *Schott and Mc-*  
27 *Creary, 2001*). The weak winds cannot overturn the stratified low-salinity surface  
28 layer and hence results into a shallow surface mixed layer. Once the strong strat-  
29 ification in the surface layer takes place, the SST is mainly driven by surface net  
30 heat flux. As a consequence, though the Arabian Sea and BoB gets almost same  
31 amount of net radiative heating, the SST over BoB is much warmer than that over  
32 Arabian Sea (*Shenoi et al., 2002*). In general, the SST of northern BoB remains  
33 higher than 28°C throughout the year, a condition favorable for generation of ac-  
34 tive convection (*Gadgil et al., 1984*; *Graham and Barnett, 1987*). SST values higher  
35 than 28°C supports large-scale deep convection in the atmosphere during the Indian  
36 summer monsoon season. **Release of latent heat due to condensation main-**  
37 **tains the atmospheric heating and sustains the monsoon circulation and**

38 **associated rainfall over Indian subcontinent (e.g. Webster et al., 1998).**  
39 Most of the studies on monsoon breaks have identified mechanisms involving various  
40 atmospheric processes as the possible reason for break monsoon conditions (*Krish-*  
41 *nan et al.*, 2000). But, oceanic parameters (like SST and salinity) also play crucial  
42 role in the evolution of break conditions (e.g. *Vecchi and Harrison*, 2002). The in-  
43 traseasonal SST changes can be associated with changes in the surface winds and  
44 atmospheric convection over BoB. On the other hand, these atmospheric changes  
45 may be responsible for the observed SST variability over the Bay. Therefore, the  
46 intraseasonal SST variability and monsoon rainfall are dynamically linked with each  
47 other (*Parampil et al.*, 2010; *Vecchi and Harrison*, 2002).

48 Fresh water from the local rainfall and river discharges maintains the low salinity  
49 surface layer over the BoB (*Parampil et al.*, 2010; *Shetye et al.*, 1996). In the  
50 Bay of Bengal Monsoon Experiment (BOBMEX) during July-August, 1999, several  
51 active and weak spells of convection occurred (*Bhat et al.*, 2001) and it was found  
52 that the SST decreases during rain events and increases in cloud free conditions.  
53 During phase-I (27<sup>th</sup> July to 6<sup>th</sup> August, 1999) of BOBMEX, the northern bay  
54 was convectively very active and three monsoon systems developed, SST remained  
55 around 28.5 °C and arrival of a low-saline water plume was reported (*Bhat*, 2002;  
56 *Vinayachandran et al.*, 2002). This plume caused the surface salinity to decrease  
57 from 33 practical salinity unit (psu) to less than 29 psu in a span of just 4 days.  
58 However, the dynamics behind the abrupt decrease in salinity is not understood  
59 completely. Phase-II of BOBMEX (13–24<sup>th</sup> August, 1999) experienced a weak phase  
60 of convection with low winds and clear sky conditions. An increase of 1.5 °C SST was  
61 observed (from 28 °C to 29.5 °C) within an interval of 5 days. *Bhat* (2002) made an  
62 one-dimensional heat budget analysis (so called calorimetric experiment) and used  
63 observed surface fluxes to predict SST. This model had limited success and could  
64 not predict SST for all conditions prevailing over northern BoB. They argued that,  
65 the horizontal advection is important for determining SST, but it was not possible to  
66 quantify the relative role of advection on the SST evolution. *Vinayachandran et al.*  
67 (2002) suggested the source of fresh water plume mainly to river discharge, which  
68 got advected from east coast due to Ekman flow and consequently accelerated due  
69 to presence of two low pressure systems over BoB. This study gave a broad overview  
70 of the source of fresh water plume, but could not localize it and cannot identify how  
71 intraseasonal oscillation of rainfall modulates this source.

72 Using in-situ observation, we have for the first time quantified the relative role of  
73 advection and surface net heat flux on the evolution of SST and salinity in northern  
74 BoB. Longer period of salinity and SST data from **R**esearch **M**oored **A**rray for  
75 **A**frican-**A**sian-**A**ustralian **M**onsoon **A**nalysis and **P**rediction (RAMA) buoy have  
76 been utilized to show that the changes in salinity are linked with the rainfall over  
77 Ganga and Brahmaputra river catchment area. Section 2 **describes** the data used  
78 for this study and applied methodology. Results are discussed in section 3. The  
79 outcomes of this study are summarized in section 4.

## 80 2 Data and Methodology

81 The Indian Climate Research Programme (ICRP) has formulated the Continental  
 82 Tropical Convergence Zone (CTCZ) programme to understand the mechanisms lead-  
 83 ing to space-time variation of the CTCZ and the embedded monsoon disturbances  
 84 during the summer monsoon. The complete overview and detailed objectives of  
 85 CTCZ programme is available at <http://www.imd.gov.in/SciencePlanofFDPs/CTCZ>.  
 86 Under this national program (CTCZ), oceanic and atmospheric observations are  
 87 taken on-board ocean research vessel (ORV) SagarKanya (SK-261). The cruise  
 88 track is shown in Figure 1. The research vessel started on 15<sup>th</sup> July 2009 from the  
 89 port of Chennai and reached the time series location (TSL) at 89°E,19°N on 22<sup>nd</sup>  
 90 July and stationed there for 15 days (up to 6<sup>th</sup> August). Two hourly profiling up  
 91 to the depth of 760 m was done for the measurement of salinity and temperature.  
 92 **Total 218 profiles were measured using Conductivity-Temperature-Depth**  
 93 **(CTD) instrument, manufactured by Idronaut.** To estimate the horizontal  
 94 advection of salinity and temperature, CTD measurement at 4 other locations situ-  
 95 ated at North, South, East and West of the TSL and at a distance of 3 nautical miles  
 96 from the TSL were carried out. In order to avoid the influence of solar insolation,  
 97 the CTD measurement at North, South, East and West locations are done once at  
 98 night and up to the depth of 150 m. The temperature and conductivity sensor of  
 99 Idronaut CTD has an accuracy of 0.001 °C and 0.0001  $Sms^{-1}$  respectively and scan  
 100 frequency is of 40 Hz. The speed of probe during downcast and up-cast was between  
 101 0.5 – 1  $m s^{-1}$ . The downcast and up-cast data were averaged into 1 m depth bins.  
 102 The tendency of temperature and salinity can be calculated by using the following  
 103 equations (*Nisha et al.*, 2009).

$$\frac{\partial T}{\partial t} = -(u \frac{\partial T}{\partial x} + v \frac{\partial T}{\partial y} + w \frac{\partial T}{\partial z}) + \frac{Q_s}{\rho C_p h} + D \quad (1)$$

$$\frac{\partial S}{\partial t} = (E - P) \frac{S}{h} - (u \frac{\partial S}{\partial x} + v \frac{\partial S}{\partial y}) + \frac{H}{h} (w_h + \frac{dh}{dt})(S - S_h) \quad (2)$$

104 where,  $T$  is the ocean water temperature,  $u, v, w$  are zonal, meridional and vertical  
 105 component of the currents,  $Q_s$  is the net surface heat flux,  $\rho$  is the density of water,  
 106  $h$  is the mixed layer depth,  $C_P = 3993.0 J kg^{-1} K^{-1}$  is the heat capacity of water,  
 107  $S$  is the salinity of water,  $E, P$  are evaporation and precipitation rate respectively.  
 108  $w_h$  is the vertical advection below mixed layer ( $m month^{-1}$ ),  $H$  is the Heaviside step  
 109 function [=0 if  $(w_h + \frac{dh}{dt}) > 0$ , =1 if  $(w_h + \frac{dh}{dt}) < 0$ ] and  $S_h$  is the salinity just below  
 110 the mixed layer base.

111 The net surface heat flux is used from NCEP reanalysis (*Kalnay et al.*, 1996). The  
 112 oceanic u,v currents are from NCEP Global Ocean Data Assimilation System (GO-  
 113 DAS, data provided by the NOAA/OAR/ESRL PSD, Boulder, Colorado, USA, from  
 114 their Web site at <http://www.esrl.noaa.gov/psd/>). High resolution oceanic currents  
 115 (Ekman and geostrophy) are derived using quick scatterometer (QuikSCAT) (Ebuchi

116 et al., 2002) wind and AVISO (Analysis, Validation and Investigation of Satellite  
 117 Oceanography) sea surface height data (Ducet et al., 2000) respectively. The Ekman  
 118 current is calculated using the following equation

$$u_{ek} = \frac{\tau^y}{f\rho_o h} \quad \text{and} \quad v_{ek} = -\frac{\tau^x}{f\rho_o h}, \quad (3)$$

where Coriolis force  $f = 2\Omega\sin\theta$ ,  $\rho_o$  = mixed layer ocean water density. wind stress  $\tau^x = \rho_a C_D u^2$  and  $\tau^y = \rho_a C_D v^2$ , with  $C_D = 1.5 \times 10^{-3}$ ,  $\rho_a = 1.252 \text{ kg m}^{-3}$ . Using sea surface height ( $H$ ) data, the geostrophic current is calculated using the following equation

$$u_g = -\frac{g}{f} \frac{\partial H}{\partial y} \quad \text{and} \quad v_g = \frac{g}{f} \frac{\partial H}{\partial x} \quad (4)$$

119 **In addition to the cruise data, we have used daily surface layer salinity,**  
 120 **temperature and rainfall measured at 15 °N, 90 °E from RAMA Buoy for**  
 121 **the period October 2008 to December 2010 (McPhaden et al., 2009).**  
 122 Daily rainfall data from GPCP are used in order to identify the large scale mon-  
 123 soon events (<http://precip.gsfc.nasa.gov/index.html>). **In addition to that, high**  
 124 **resolution daily rainfall data from 3B42 (Huffman et al., 1995, 2007) for**  
 125 **the period 1<sup>st</sup> June to 31<sup>st</sup> December 2009 are used.**

## 126 3 Results

### 127 3.1 Observed Features

128 **Time series location witnessed three rainfall events; first one on 24 – 25<sup>th</sup>**  
 129 **July, second on 27 – 28<sup>th</sup> July and third on 2 – 5<sup>th</sup> August (Figure 2a).**  
 130 **The cruise left the TSL location on 6<sup>th</sup> August at noon, therefore rainfall**  
 131 **data of that day is not complete. However, rainfall from 3B42 shows the**  
 132 **last event continued till 9<sup>th</sup> August (Figure not shown). Since there are**  
 133 **no clear gap between 1<sup>st</sup> and 2<sup>nd</sup> event, together they can be considered**  
 134 **as an active phase of monsoon intraseasonal oscillation (ISO) with peak**  
 135 **around 27 – 28<sup>th</sup> July and the second active phase with peak around 5 – 6<sup>th</sup>**  
 136 **August.** Temperature and salinity profile up to 100 *m* depth and their evolution  
 137 during 15 days at TSL location are shown in Figures 2b, 2c respectively. Prior to  
 138 the beginning of rainfall activity, the SST increased to 28.5 °C for a brief period  
 139 of about 2 days (23 – 24<sup>th</sup> July, Figure 2a). A rapid decrease in surface layer  
 140 salinity is observed during 29 – 30<sup>th</sup> July. After the initiation of freshening, the  
 141 water temperature at the surface layer (10 – 15 *m*) remained always above 28.5 °C.  
 142 Furthermore, from 30<sup>th</sup> July onward the salinity of top 10 – 15 *m* layer maintained

143 at minimum value and that level coincides with the warm water ( $\geq 28.5^\circ\text{C}$ ) layer  
 144 at the top. The average mixed layer salinity (depth) between 22 – 28<sup>th</sup> July is  
 145 32.4 *psu* (30.72 *m*) and the average between 31<sup>st</sup> July to 6<sup>th</sup> August is 28.07 *psu*  
 146 (6.297 *m*). The salinity dropped by more than 4 *psu* within the 24 hours (Figure  
 147 2f). Changes in temperature of mixed layer also took place almost at the same time.  
 148 The average mixed layer temperature during 22 – 28<sup>th</sup> July (31<sup>st</sup> July - 6<sup>th</sup> August)  
 149 is 28.45 °C (28.81 °C). The mixed layer depth (MLD) started shoaling immediately  
 150 after the first active phase and continued to shoal until end of the cruise (Figure  
 151 2d). Similarly the barrier layer thickness started to deepen immediately after the  
 152 first active phase of rainfall. Similar decrease in sea surface salinity (SSS) was also  
 153 observed by *Bhat* (2002) in BOBMEX experiment (*Bhat et al.*, 2001) in its phase  
 154 1, where SSS decreased from 33 *psu* to 29 *psu* during 27<sup>th</sup> July to 3<sup>rd</sup> August 1999  
 155 and remained low for the rest observation period. **During BOBMEX salinity**  
 156 **dropped gradually (4 *psu* in 7 days), while during CTCZ cruise similar**  
 157 **amount of salinity dropped within 24 hours.** Therefore, it is very interesting  
 158 to understand the mechanism behind rapid decrease of salinity during CTCZ cruise.

### 159 3.2 Heat and Salt Budget

160 The estimated temperature tendency at TSL using GODAS currents are able to  
 161 capture the observed tendency reasonably well (Figure 3a). The mixed layer tem-  
 162 perature is controlled equally by both, advection and net surface heat flux. As from  
 163 30<sup>th</sup> July onward the mixed layer salinity started to fall, the advection of fresh and  
 164 cold water decreases the temperature. **On the other hand, the net surface heat**  
 165 **flux (mainly the radiative flux) causes extreme warming, probably due**  
 166 **to presence of shallow barrier layer (Figure 2d).** Since the mixed layer depth  
 167 became shallow, the net surface heat flux became very effective in increasing tem-  
 168 perature. The salinity budget analysis reveals that advection is the major source of  
 169 fresh water at TSL and the sudden fall in salinity on 29 – 30<sup>th</sup> July is mainly due to  
 170 advected fresh water (figure 3b). The **change** in salinity due local fresh water flux  
 171 (i.e. E-P) is very small. Similar analysis using estimated Ekman and geostrophic  
 172 current closes the heat and salinity budgets quite well till 29<sup>th</sup> July and afterward  
 173 the advection of salinity and temperature is too strong (not shown). The reasons for  
 174 overestimation of advection due to Ekman and geostrophic currents are not clear.  
 175 The estimated geostrophic currents derived from sea surface height (from satellites  
 176 and in-situ data) over estimate the advection component of budget. Using data col-  
 177 lected during BOBMEX expedition, *Vimayachandran et al.* (2002) concluded that  
 178 wind driven circulation i.e. Ekman current **determines** the path of fresh water in  
 179 the BoB. They further concluded that fresh water advected eastward from the coast  
 180 of India to the study location at 17.5 °N, 89 °E. However, during our observational  
 181 period the average mixed layer current in GODAS reanalysis was always **south-**  
 182 **ward and south-westward** (Figure 3c). On the other hand, the estimated total  
 183 current were **south-westward** when the budgets are almost closed (i.e. till 29<sup>th</sup>

184 July) and became **south-eastern** afterward when the budget is not closed (figure  
185 not shown). The river discharge from the north coast is much higher (Ganga and  
186 Brahmaputra) compared to the east coast (Mahanadi, Godavari, Krishna and Cau-  
187 very) (*Rao and Sivakumar, 2003*). **It is plausible that if advection of fresh**  
188 **water takes place from north, the freshening will be larger compared to**  
189 **cases when advection is from the east coast of India.** Therefore, it is evident  
190 from the above analysis that, southward current tends to close the heat and salinity  
191 budget reasonably well and hence, freshwater may have advected mainly from the  
192 north (i.e. discharged from Ganga and Brahmaputra rivers). This can explain the  
193 rapid (slow) decrease in salinity during CTCZ (BOBMEX) cruise.

### 194 3.3 Intraseasonal Variability

195 Using in-situ data at the TSL, it is not possible to know whether the freshening  
196 continued throughout the monsoon season with the same level. If the freshening is  
197 dominated by river discharge, the monsoon ISO signal may be present in the surface  
198 layer salinity with certain time lag and this can modulate the surface layer tempera-  
199 ture. Since long term data are not available to address the above, we have selected a  
200 close by buoy data for this purpose. RAMA buoy data at  $90^{\circ}\text{E}, 15^{\circ}\text{N}$  (**south-east**  
201 **of TSL; Figure 1**) have longer observation period and indeed it shows oscillation in  
202 the surface layer salinity during monsoon period and beyond (Figure 4b). **It may be**  
203 **noted that a sudden freshening started at the beginning of October 2009**  
204 **and continued for the next few month with some variability. However,**  
205 **the local rainfall is quite negligible and hence change in salinity cannot**  
206 **be explained through local fresh water flux (i.e E-P). Such variability in**  
207 **salinity/SST are not unique, but also observed in other years (i.e. 2008**  
208 **and 2010) as evident from available continuous observation for the period**  
209 **October 2008 to December 2010 (Figure 4b, 4c).** Simultaneous response in  
210 surface layer warming is also evident (Figure 4c). **Power spectrum analysis of**  
211 **June-December 2009 salinity (temperature) averaged over top 35 m shows**  
212 **significant variance at around 13 (15) days. Other significant peaks in**  
213 **salinity and temperature are found between 30-60 days period (Figure 5).**  
214 **SST also shows significant peak quite similar to that of 35 m average water**  
215 **temperature (figure not shown).** These two preferred band are similar to the  
216 summer monsoon rainfall variability on the intraseasonal time scale (i.e. 10-20 and  
217 30-60 days mode). Similarly two epochs of rainfall during CTCZ cruise are also sep-  
218 arated by 10 days. Power spectrum analysis using GPCP rainfall, averaged around  
219 TSL ( $87^{\circ}\text{-}92^{\circ}\text{E}, 17^{\circ}\text{-}21^{\circ}\text{N}$ ) for 2009 summer monsoon season (JJAS) shows signifi-  
220 cant power at 12.5 days period (figure not shown). Therefore, the observed rainfall  
221 activity belongs to quasi bi-weekly (10-20 days) mode of intraseasonal oscillation,  
222 which in general propagates westward (*Chatterjee and Goswami, 2004*).

223 In order to find out the maximum rainfall variability region and to relate it with the

224 observed salinity, **variance of 10-100 days filtered rainfall anomaly (June-**  
225 **December 2009)** are calculated. The heavy rainfall regions due to monsoon  
226 ISOs are depicted by large variance (Figure 6). Therefore, there is possibility that  
227 fresh water of those region may modify the salinity either locally or through ad-  
228 vection processes. Thus, four regions (D1, D2, D3, D4) are identified based on the  
229 larger rainfall variance which may modify the salinity at the location of RAMA  
230 buoy on monsoon rainfall ISO time scale (Figure 6). Domain D1 (86°- 93°E, 22°-  
231 27°N) and D2 (79°- 87°E, 18°- 23°N) represent the river catchment area of Ganga,  
232 Brahmaputra and Mahanadi. D3 (88°- 95°E, 12°- 19°N) represent the area over  
233 BoB with maximum rainfall ISO variance and the RAMA buoy is located within  
234 this box. D4 (88°- 92°E, 13°- 17°N) represent the smaller domain surrounding the  
235 RAMA buoy and it also covers part of maximum rainfall ISO variance region.

236 Power spectrum analysis of rainfall averaged over individual domain shows signifi-  
237 cant variances at 3-7 days time scale except in D1, where the significant variances  
238 are at around 10 days (Figure 7). **In addition to that, rainfall at D1 shows**  
239 **significant variability at about 50 days period. Similar analysis of sur-**  
240 **face layer salinity and temperature (top 35m average) at RAMA buoy**  
241 **also reveals the prominence of power at the ISO bands (Figure 5). Thus**  
242 **both rainfall over domain D1 and salinity at RAMA buoy has the dom-**  
243 **inance on the ISO time scale, which imply that rainfall over D1 may**  
244 **affect salinity at RAMA buoy in a delayed mode and at the same time,**  
245 **the local rainfall as well as river discharged water from Indian east coast**  
246 **can't explain the observed salinity variability. Cross spectrum analysis of**  
247 **rainfall at D1 and salinity for the period June to December 2009 further**  
248 **reveals large coherence at 10 and 50 days time scale and rainfall leads**  
249 **the salinity by about 60 days (Figure 8). Similar analysis using rainfall**  
250 **of other domain shows maximum coherence at synoptic time scale (3-7**  
251 **days) and hence can't explain the variation of salinity on ISO time scale.**  
252 **To advect fresh water from the TSL to RAMA buoy, the average speed of**  
253 **southerly current should be about  $8.75\text{ cm s}^{-1}$ , which is within the range**  
254 **of observed southerly current. Therefore, it is very likely that the first**  
255 **pulse of observed freshening at TSL may have advected towards south**  
256 **and reached RAMA buoy location on the beginning of October 2009.**

257 To further confirm this possibility in detail we have used Wavelet analysis (*Grinsted*  
258 *et al.*, 2004). It is a powerful tool giving both the information of the dominant mode  
259 of variability in spectral domain and their exact occurrences in time domain. Cross  
260 wavelet transform (CWT) has been performed between salinity at RAMA buoy and  
261 rainfall averaged over **D1 for the time period 1<sup>st</sup> June 2009 to 28<sup>th</sup> February**  
262 **2010.** Significant common power on 10-20 days mode are observed twice viz. 15<sup>th</sup>  
263 July to 15<sup>th</sup> August and 10<sup>th</sup> September to 20<sup>th</sup> October (Figure 9a). Phase angle  
264 during July-August period suggests that the salinity change was almost simultaneous  
265 with the rainfall over D1. This further indicates that rainfall over both the location  
266 is from the active phase of ISO, which occurred almost simultaneously over northern



267 BoB as well as over D1. However during September-October, the rainfall and salinity  
268 are in opposite phase. Hence, sudden freshening at the beginning of month October  
269 is directly related with the rainfall over D1 which took place earlier. The squared  
270 wavelet coherence (WC) also shows significant coherence on 10-20 days time scale  
271 during September-October (Figure 9b). This indeed shows that sudden freshening at  
272 RAMA buoy on the beginning of October is due to rainfall at D1 and the same fresh  
273 water is observed first at TSL and subsequently at the buoy location. **Significant**  
274 **coherence is also evident on 30-60 days band during month of August to**  
275 **September. Therefore, salinity at RAMA buoy is affected by rainfall at**  
276 **D1 from both mode of ISOs.**

277 **In order to bring out a clear picture of lead/lag relation between salin-**  
278 **ity and rainfall, filtered salinity anomaly at RAMA buoy are linearly**  
279 **regressed with filtered rainfall and current anomalies (estimated) of all**  
280 **other points. Here, 10-100 days and 30-60 days Lanczos band pass fil-**  
281 **ter are used. Regressed anomalies averaged over 88°-92°E (Figure 10)**  
282 **show a clear southward propagation of fresh water and it takes about**  
283 **50-60 days to reach RAMA buoy from D1. Rainfall regressed with SST**  
284 **at RAMA also shows similar lead/lag relation (Figure not shown). Fur-**  
285 **thermore, regressed current anomaly shows strong southerly component**  
286 **(Figure 11), which implies southward advection of river discharged fresh**  
287 **water through oceanic currents. As evident from spectrum analysis, the**  
288 **30-60 days mode has large variance and as a consequence all the regressed**  
289 **anomalies are stronger on the same ISO band.**

## 290 4 Summary and Conclusions

291 Under the CTCZ program, oceanic and atmospheric observations are taken on-  
292 board ORV SagarKanya. She started on 15<sup>th</sup> July 2009 from the port of Chennai  
293 and reached the TSL on 22<sup>nd</sup> July and stayed there up to 6<sup>th</sup> August. In every  
294 2 hours of interval, salinity and temperature profile up to the depth of 760 m was  
295 measured. Total 218 profiles were measured using **Idronaut** CTD. To estimate  
296 the horizontal advection of salinity and temperature, CTD measurement at 4 other  
297 locations situated at North, South, East and West of the TSL and at a distance of  
298 3 nautical miles from the TSL are carried out.

299 A sudden freshening is observed during 29–30<sup>th</sup> July, where the mixed layer averaged  
300 salinity dropped by more than 4 *psu* within 24 hours time. A simultaneous increase  
301 in mixed layer averaged temperature by 0.36 °C is also observed. The budget analysis  
302 of salinity and heat primarily indicates dominant role of advection processes on  
303 temperature and salinity at the northern BoB. As the local rainfall contribution to  
304 the salinity change was meager, the freshening can only be explained through the  
305 southerly Ekman flow which advected river discharged water from the north. Even

306 though previous studies expected that due to strong stratification, heat budget into  
307 northern BoB can be considered as one dimensional problem, we have presented an  
308 evidence that advection also plays a major role.

309 **Daily salinity and temperature data (averaged over top 35m) at south-**  
310 **east of TSL from RAMA (90 °E, 15 °N) reveals significant variance at time**  
311 **scale which falls within the 10-20 days bands of monsoon ISO. Again, the**  
312 **local rainfall is not large enough to explain the salinity change. Among**  
313 **the different catchment area, only rainfall at Ganga-Brahmaputra catch-**  
314 **ment areas shows maximum coherence at 10 and 50 days time scale**  
315 **with lag of about 60 days. Wavelet co-spectrum and coherence analy-**  
316 **sis of above two time series further reveals significant power and max-**  
317 **imum resonance respectively at 10-20, and 30-60 days time scale dur-**  
318 **ing September-October. Anti phase relation between time series of salinity at**  
319 **RAMA location and rainfall over Ganga-Brahmaputra river catchment area further**  
320 **suggests that intraseasonal variation of salinity is mainly due to river runoff and**  
321 **the same varies with the monsoon rainfall ISO over river catchment areas. Re-**  
322 **gressed rainfall, oceanic current with salinity and temperature at RAMA**  
323 **buoy illustrate the southward advection of fresh water from the Ganga-**  
324 **Brahmaputra river catchment area on ISO time scale.**

325 This study aids in further our understanding of ocean advection, playing a crucial  
326 role in forming barrier layer and thus modifying SST significantly. Thus providing  
327 a different perspective in terms of lagged response of salinity which dictates the  
328 convective activity over BoB during the withdrawal and post monsoon phases. **Most**  
329 **of the climate models prescribe fixed amount of river discharge. As a**  
330 **result models may not be able to capture the post-monsoon SST/SSS**  
331 **variability merely due to the lagged response of rainfall over Ganga-**  
332 **Brahmaputra catchment area and hence may affect the genesis of post-**  
333 **monsoon cyclone over BoB.**

334

## 335 Acknowledgments

336 The authors acknowledge the financial support from Department of Science and  
337 Technology (DST) under the research project “Oceanographic Observations in the  
338 northern Bay of Bengal deep convection during CTCZ”. Freeware Ferret and Grads  
339 is used extensively in this study. The GPCP one-degree daily precipitation data set  
340 were provided by the NASA/Goddard Space Flight Center’s Laboratory for Atmo-  
341 spheres, which develops and computes the 1 °data as a contribution to the GEWEX  
342 Global Precipitation Climatology Project. **We thank three anonymous review-**

343 ers for their constructive comments to improve the previous version of  
344 this manuscript.

## 345 References

- 346 Bhat, G. S., Near-surface variations and surface fluxes over the northern Bay  
347 of Bengal during the 1999 Indian summer monsoon, *J. Geophys. Res.*, *107*,  
348 4336,doi:10.1029/2001JD000382, 2002.
- 349 Bhat, G. S., S. Gadgil, P. V. H. Kumar, S. R. Kalsi, P. Madhusoodanan, V. S. N.  
350 Murty, C. V. K. P. Rao, V. R. Babu, L. V. G. Rao, R. R. Rao, M. Ravichandran,  
351 K. G. Reddy, P. S. Rao, D. Sengupta, D. R. Sikka, J. Swain, and P. N. Vinayachan-  
352 dran, BOBMEX: The Bay of Bengal Monsoon Experiment, *Bul. Amer. Meteor.*  
353 *Soc.*, *82*, 2217 – 2243, 2001.
- 354 Chatterjee, P., and B. N. Goswami, Structure, genesis and scale selection of the  
355 tropical quasi-biweekly mode, *Q. J. R. Meteorol. Soc.*, *130*, 1171–1194, 2004.
- 356 Gadgil, S., P. V. Joseph, and N. V. Joshi, Ocean atmosphere coupling over monsoon  
357 regions, *Nature*, *312*, 141 – 143, 1984.
- 358 Graham, N. E., and T. P. Barnett, Sea surface temperature, surface wind divergence,  
359 and convection over tropical oceans, *Nature*, *238*, 657 – 659, 1987.
- 360 Grinsted, A., J. C. Moore, and S. Jevrejeva, Application of the cross wavelet trans-  
361 form and wavelet coherence to geophysical time series, *Nonlin. Proc. Geophys.*, *11*,  
362 561–566, 2004.
- 363 Huffman, G. J., R. F. Adler, D. T. Bolvin, G. Gu, E. J. Nelkin, K. P. Bowman,  
364 Y. Hong, E. F. Stocker, and D. B. Wolff, The TRMM Multi-satellite Precipitation  
365 Analysis: Quasi-Global, Multi-Year, Combined-Sensor Precipitation Estimates at  
366 Fine Scale, *8*, 38 – 55, 2007.
- 367 Huffman, G. J., R. F. Adler, B. Rudolph, U. Schneider, and P. Keehn, Global Precip-  
368 itation Estimates Based on a Technique for Combining Satellite-Based Estimates,  
369 Rain Gauge Analysis, and NWP Model Precipitation Information, *J. Clim.*, *8*,  
370 1284 – 1295, 1995.
- 371 Kalnay, E., M. Kanamitsu, R. Kistler, W. Collins, D. Deaven, L. Gandin, M. Iredell,  
372 S. Saha, G. White, J. Woollen, Y. Zhu, A. Leetmaa, R. Reynolds, M. Chelliah,  
373 W. Ebisuzaki, W. Higgins, J. Janowiak, K. C. Mo, C. Ropelewski, J. Wang,  
374 R. Jenne, , and D. Joseph, The NCEP/NCAR 40-year reanalysis project, *Bul.*  
375 *Amer. Meteor. Soc.*, *77*, 437–470, 1996.
- 376 Krishnan, R., C. Zhang, and M. Sugi, Dynamics of Breaks in the Indian Summer  
377 Monsoon, *J. Atmos. Sci.*, *57*, 1354–1372, 2000.
- 378 McCreary, J. P., P. K. Kundu, and R. Molinari, A numerical investigation of dy-  
379 namics, thermodynamics and mixed-layer processes in the Indian Ocean, *Prog.*  
380 *Oceanogr.*, *31*, 181 – 244, 1993.

- 381 McPhaden, M. J., G. Meyers, K. Ando, Y. Masumoto, V. S. N. Murty, M. Ravichan-  
382 dran, F. Syamsudin, J. Vialard, L. Yu, and W. Yu, RAMA The Research Moored  
383 Array for AfricanAsianAustralian Monsoon Analysis and Prediction, *Bul. Amer.*  
384 *Meteor. Soc.*, *90*, 459 – 480, 2009.
- 385 Nisha, K., S. A. Rao, V. V. Gopalakrishna, R. R. Rao, M. S. Girishkumar, T. P. M.  
386 Ravichandran, S. Rajesh, K. Girish, Z. Johnson, M. Anuradha, S. S. M. Gavaskar,  
387 V. Suneel, and S. M. Krishna, Reduced Near-Surface Thermal Inversions in 200506  
388 in the Southeastern Arabian Sea (Lakshadweep Sea), *J. Phys. Oceanogr.*, *39*, 1184  
389 – 1199, 2009.
- 390 Parampil, S. R., A. Gera, M. Ravichandran, and D. Sengupta, Intraseasonal re-  
391 sponse of mixed layer temperature and salinity in the Bay of Bengal to heat and  
392 freshwater flux, *J. Geophys. Res.*, *115*, doi:10.1029/2009JC005790, 2010.
- 393 Rao, R. R., and R. Sivakumar, Seasonal variability of sea surface salinity and salt  
394 budget of the mixed layer of the north Indian Ocean, *J. Geophys. Res.*, *108*, 3009,  
395 doi:10.1029/2001JC000907, 2003.
- 396 Schott, F. A., and J. P. McCreary, The monsoon circulation of the Indian Ocean,  
397 *Prog. Oceanogr.*, *51*, 1 – 123, 2001.
- 398 Shenoi, S. S. C., D. Shankar, and S. R. Shetye, Differences in heat budgets of  
399 the near-surface Arabian Sea and Bay of Bengal: Implications for the summer  
400 monsoon, *J. Geophys. Res.*, *107*, 3052, doi:10.1029/2000JC000679, 2002.
- 401 Shetye, S. R., A. D. Gouveia, D. Shankar, S. S. C. Shenoi, P. N. Vinayachandran,  
402 D. Sundar, G. S. Michael, and G. Nampoothiri, Hydrography and circulation in  
403 the western Bay of Bengal during the northeast monsoon, *J. Geophys. Res.*, *101*,  
404 4011 – 14025, 1996.
- 405 Sprintall, J., and M. Tomczak, Evidence of the barrier layer in the surface layer of  
406 the tropics, *J. Geophys. Res.*, *97*, 7305 – 7316, 1992.
- 407 Vecchi, G. A., and D. E. Harrison, Monsoon breaks and subseasonal sea surface  
408 temperature variability in the Bay of Bengal, *J. Clim.*, *15*, 1485 – 1493, 2002.
- 409 Vinayachandran, P. N., V. S. N. Murthy, and V. R. Babu, Observations of barrier  
410 layer formation in the Bay of Bengal during summer monsoon, *J. Geophys. Res.*,  
411 *107*, doi:10.1029/2001JC000831, 2002.
- 412 Webster, P. J., V. O. Magaa, T. N. Palmer, J. Shukla, R. A. Tomas, M. Yanai, and  
413 T. Yasunari, Monsoons: Processesp, redictability, and the prospects for predic-  
414 tion, *J. Geophys. Res.*, *103*, 14451 – 14510, 1998.

415 **List of Figures**

416 1 Cruise track (yellow lines). Shaded color shows the climatology of  
417 surface salinity (JJAS). . . . . 15

418 2 Rainfall, temperature and salinity profile measured on-board ORV  
419 Sagar Kanya at TSL a) Rainfall in  $mm\ day^{-1}$  (black line). Rainfall  
420 events in every 2 hour interval are observed (rain or no-rain) and  
421 marked by red bars. b) Temperature of top 100  $m$  layer. Isoline of  
422  $28.5\ ^\circ C$  is marked by black contour. c) Salinity of top 100  $m$  layer in  
423 psu. d) Mixed layer depth (in meter) and barrier layer thickness (in  
424 meter). Time series of MLD averaged e) temperature and f) salinity. . 16

425 3 Salinity and temperature budget at TSL using heat flux from NCEP,  
426 surface currents from GODAS and in-situ measurement of rainfall,  
427 salinity and temperature. Observed and estimated a) temperature  
428 tendency, b) salinity tendency, c) top 20  $m$  and time averaged ( $22^{nd}$  July-  
429  $6^{th}$  August) current from GODAS. . . . . 17

430 4 Rainfall, temperature and salinity profile measured at RAMA buoy  
431 location ( $15\ ^\circ N$ ,  $90\ ^\circ E$ ) a) Rainfall in  $mm\ day^{-1}$ . b) Salinity of top  
432 100  $m$  layer in psu. c) Temperature of top 100  $m$  layer. Isoline of  
433  $28.5\ ^\circ C$  is marked by black contour. . . . . 18

434 5 Spectra of surface layer (top 35  $m$  average) a) temperature and b)  
435 salinity using RAMA buoy data at  $15\ ^\circ N$ ,  $90\ ^\circ E$  for the time period  
436  $1^{st}$  June to  $31^{st}$  **December** 2009. Red and blue curve represent 5%  
437 and 95% “red noise” confidence bounds. Smoothing of 7 days and  
438 0.3 percent taper are used. . . . . 19

439 6 Variance of 10-100 days filtered rainfall anomaly from 3B42 data (in  
440  $mm^2\ day^{-2}$ ) of the period  $1^{st}$  **June** to  $31^{st}$  **December** 2009. . . . . 20

441 7 Spectra of rainfall time series ( $1^{st}$  June to  $31^{st}$  **December** 2009) using  
442 daily 3B42RT data and averaged over a) D1 ( $86\ ^\circ - 93\ ^\circ E$ ,  $22\ ^\circ - 27\ ^\circ N$ ),  
443 b) D2 ( $79\ ^\circ - 87\ ^\circ E$ ,  $18\ ^\circ - 23\ ^\circ N$ ), c) D3 ( $88\ ^\circ - 95\ ^\circ E$ ,  $12\ ^\circ - 19\ ^\circ N$ ), d) D4  
444 ( $88\ ^\circ - 92\ ^\circ E$ ,  $13\ ^\circ - 17\ ^\circ N$ ). Red and blue curve represent 5% and 95%  
445 “red noise” confidence bounds. . . . . 21

446 8 a) Coherence and b) phase angle between rainfall averaged over do-  
447 main D1 ( $86\ ^\circ - 93\ ^\circ E$ ,  $22\ ^\circ - 27\ ^\circ N$ ) and salinity at RAMA buoy ( $15\ ^\circ N$ ,  
448  $90\ ^\circ E$ ) for the time period  $1^{st}$  June to  $31^{st}$  **December** 2009. . . . . 22

449	9	a) Wavelet co-spectrum and b) squared wavelet coherence between	
450		rainfall (averaged over D1) and salinity at RAMA buoy (top 35m	
451		averaged) for the period June-December 2009. Thick contour shows	
452		the area significant at 95% level and arrow indicates the phase angle	
453		between these two time series. . . . .	23
454	10	Lag-latitude section (88°-92°E average) of regressed rainfall anom-	
455		alies over D1 with top 35 m average salinity at RAMA buoy (1 <sup>st</sup> June-	
456		31 <sup>st</sup> December 2009). a) 10-100 days filtered anomalies, b) 30-60 days	
457		filtered anomalies. . . . .	24
458	11	Regressed estimated current anomaly with top 35 m average salinity	
459		at RAMA buoy (1 <sup>st</sup> June-31 <sup>st</sup> October 2009). a) 10-100 days filtered	
460		Ekman current, b) 30-60 days filtered Ekman current, c) 10-100 days	
461		filtered total (Ekman + Geostrophy) current, d) 30-60 days filtered	
462		total current. . . . .	25

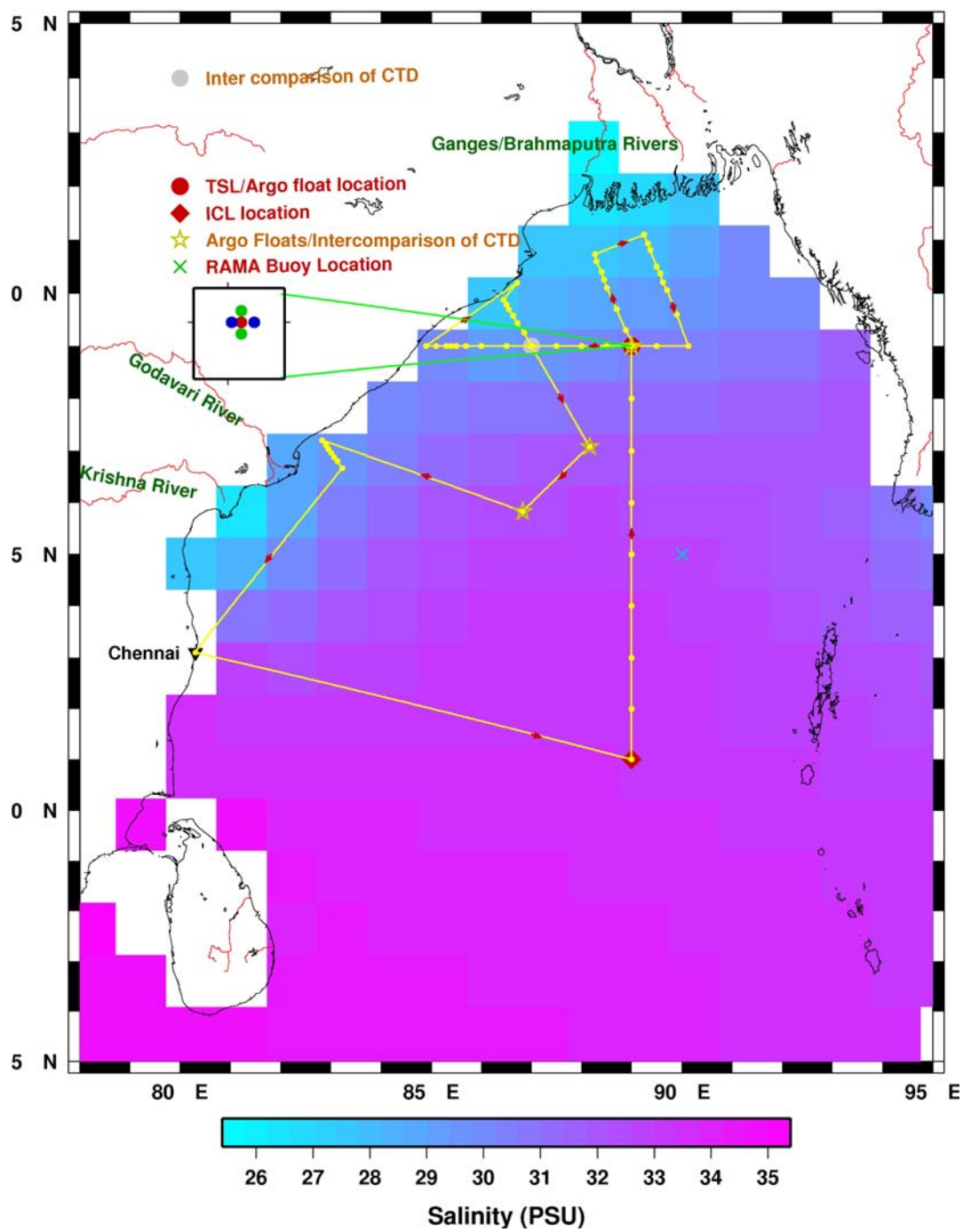


Figure 1: Cruise track (yellow lines). Shaded color shows the climatology of surface salinity (JJAS).



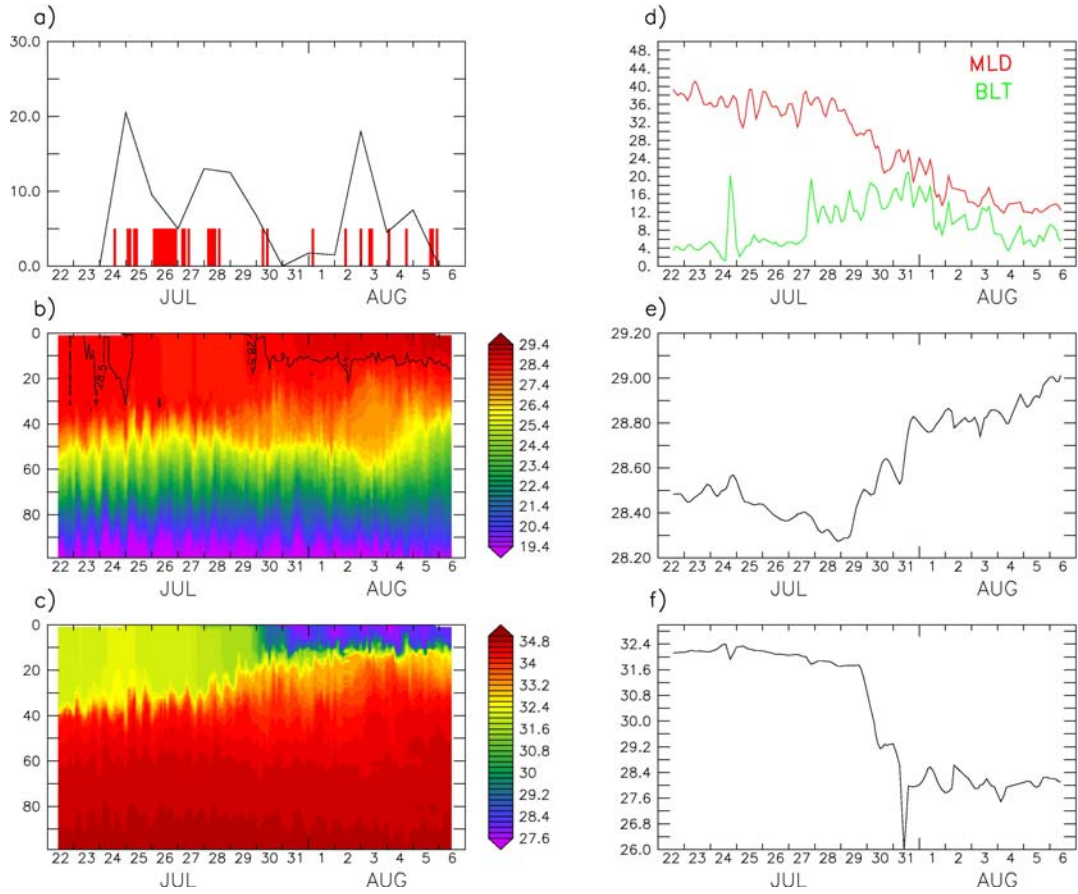


Figure 2: Rainfall, temperature and salinity profile measured on-board ORV Sagar Kanya at TSL a) Rainfall in  $mm\ day^{-1}$  (black line). Rainfall events in every 2 hour interval are observed (rain or no-rain) and marked by red bars. b) Temperature of top 100 m layer. Isoline of 28.5  $^{\circ}C$  is marked by black contour. c) Salinity of top 100 m layer in psu. d) Mixed layer depth (in meter) and barrier layer thickness (in meter). Time series of MLD averaged e) temperature and f) salinity.

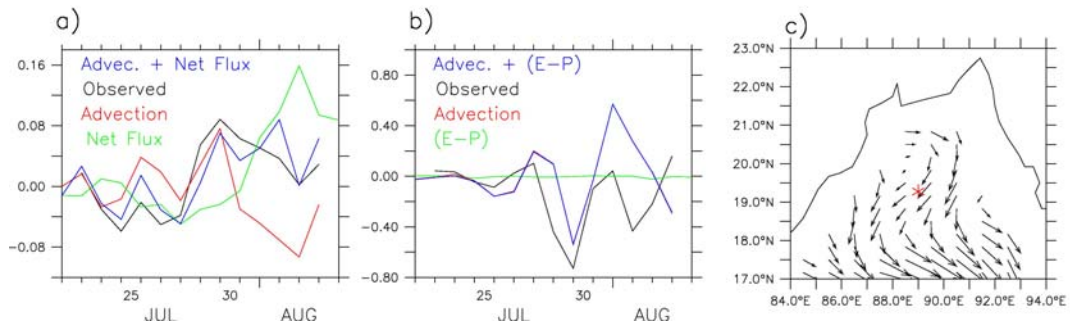


Figure 3: Salinity and temperature budget at TSL using heat flux from NCEP, surface currents from GODAS and in-situ measurement of rainfall, salinity and temperature. Observed and estimated a) temperature tendency, b) salinity tendency, c) top 20 m and time averaged (22<sup>nd</sup> July-6<sup>th</sup> August) current from GODAS.

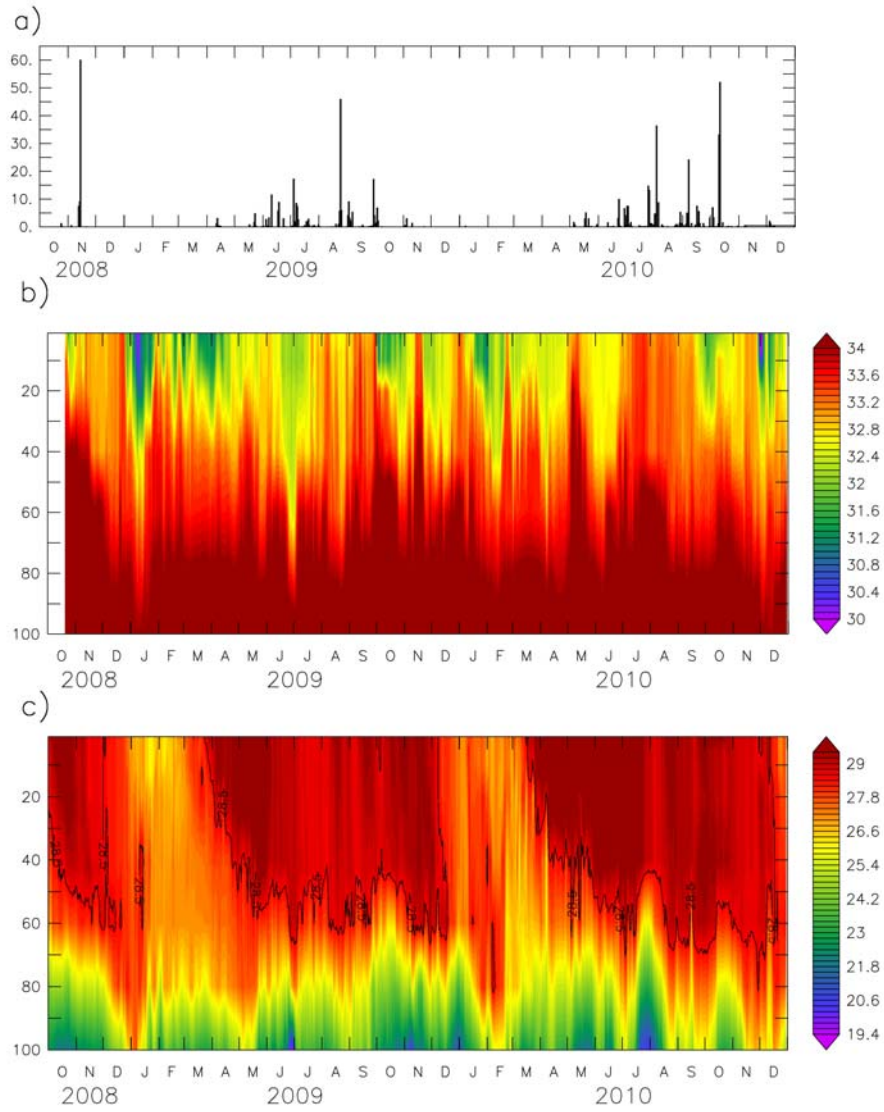


Figure 4: Rainfall, temperature and salinity profile measured at RAMA buoy location ( $15^{\circ}N$ ,  $90^{\circ}E$ ) a) Rainfall in  $mm\ day^{-1}$ . b) Salinity of top 100 m layer in psu. c) Temperature of top 100 m layer. Isoline of  $28.5^{\circ}C$  is marked by black contour.

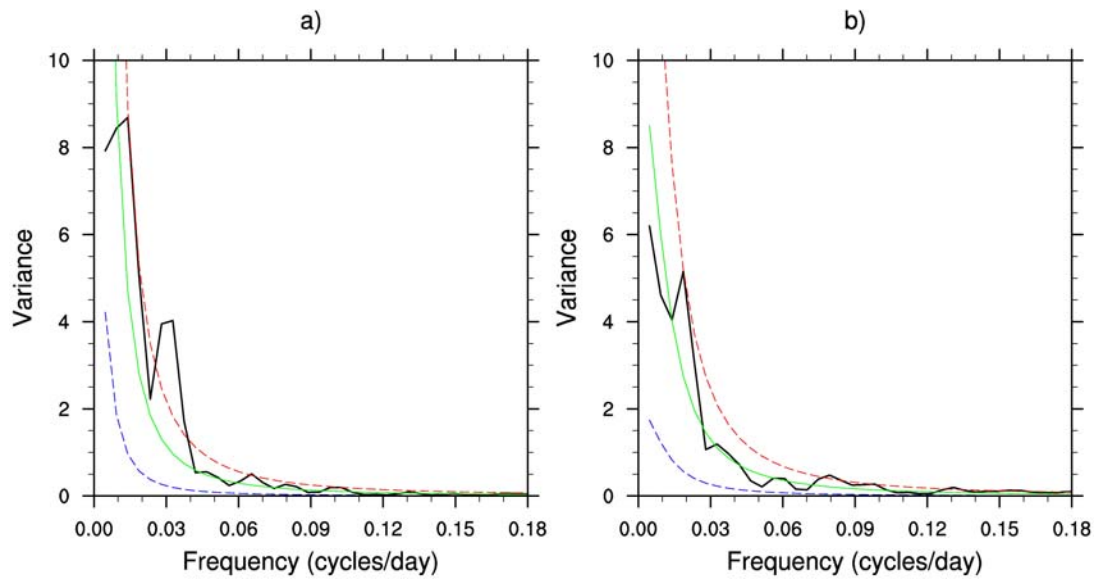


Figure 5: Spectra of surface layer (top 35 *m* average) a) temperature and b) salinity using RAMA buoy data at 15°N, 90°E for the time period 1<sup>st</sup> June to 31<sup>st</sup> **December** 2009. Red and blue curve represent 5% and 95% “red noise” confidence bounds. Smoothing of 7 days and 0.3 percent taper are used.

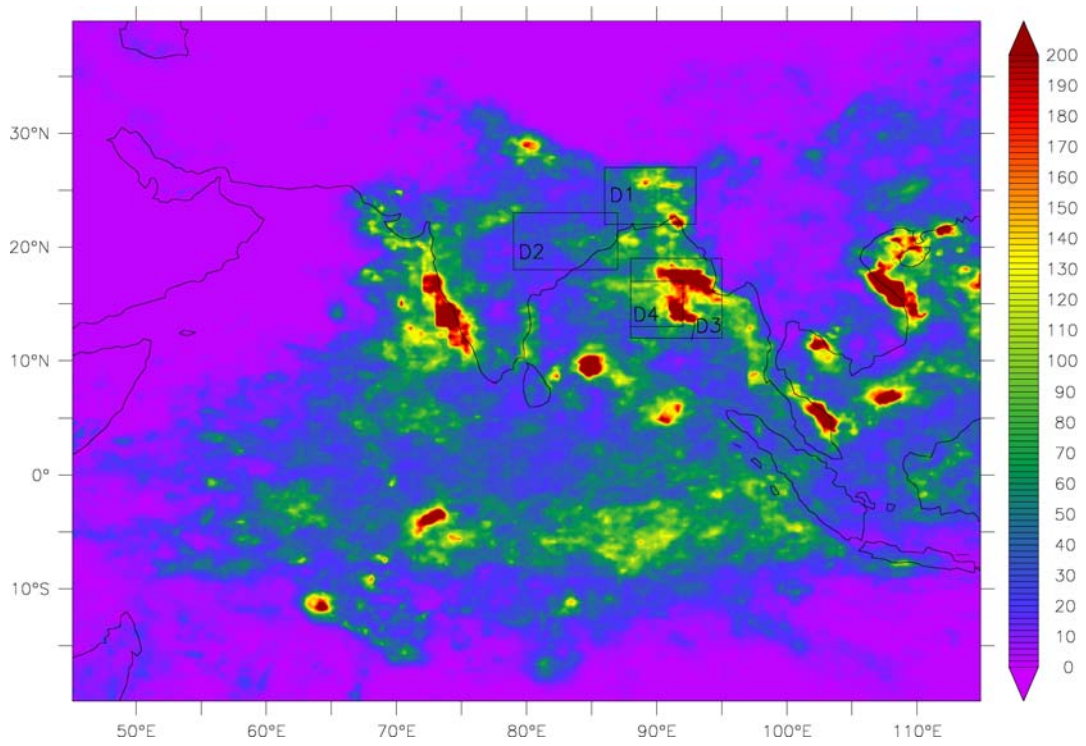


Figure 6: Variance of 10-100 days filtered rainfall anomaly from 3B42 data (in  $mm^2 day^{-2}$ ) of the period 1<sup>st</sup> **June** to 31<sup>st</sup> **December** 2009.

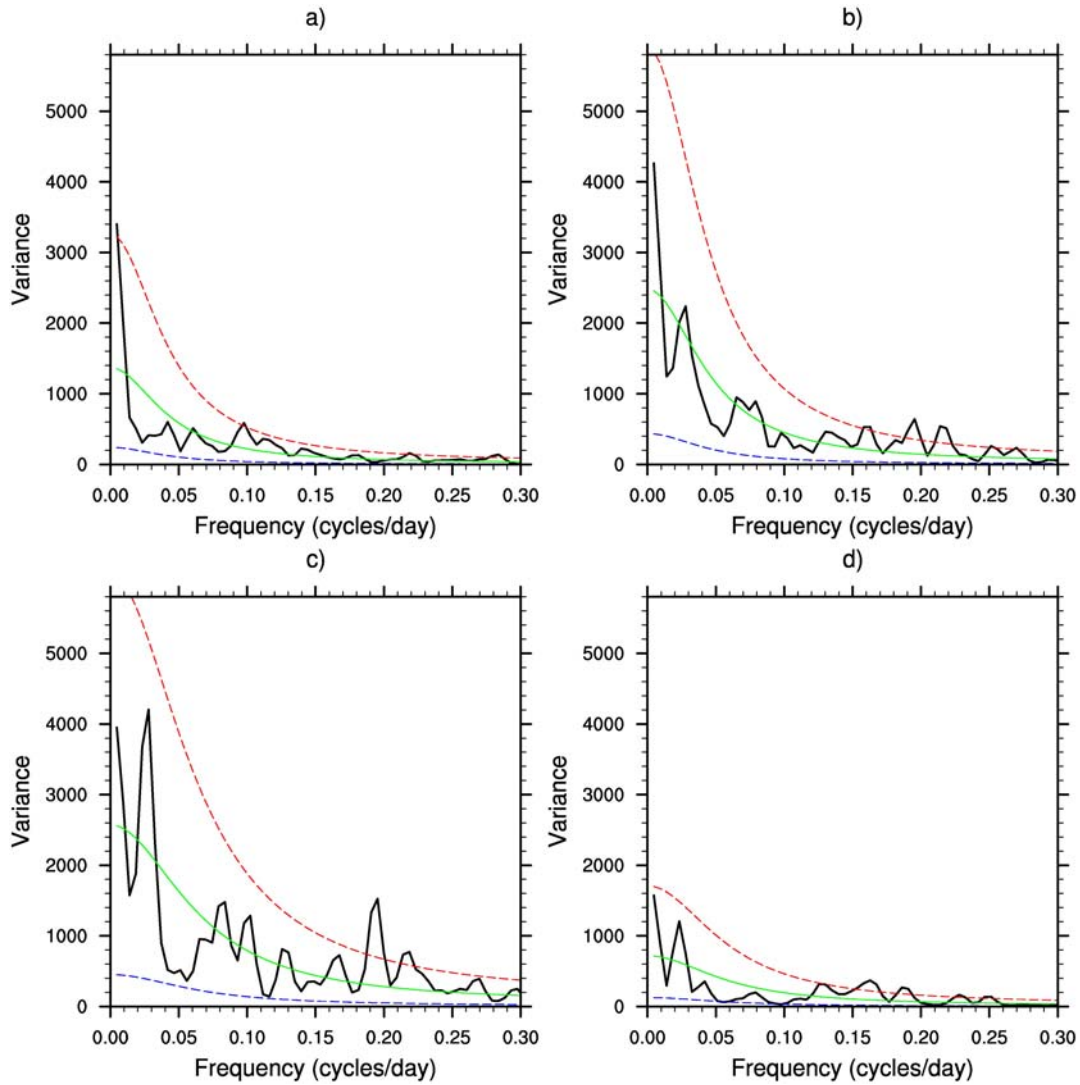


Figure 7: Spectra of rainfall time series (1<sup>st</sup> June to 31<sup>st</sup> **December** 2009) using daily 3B42RT data and averaged over a) D1 (86°- 93°E, 22°- 27°N), b) D2 (79°- 87°E, 18°- 23°N), c) D3 (88°- 95°E, 12°- 19°N), d) D4 (88°- 92°E, 13°- 17°N). Red and blue curve represent 5% and 95% “red noise” confidence bounds.

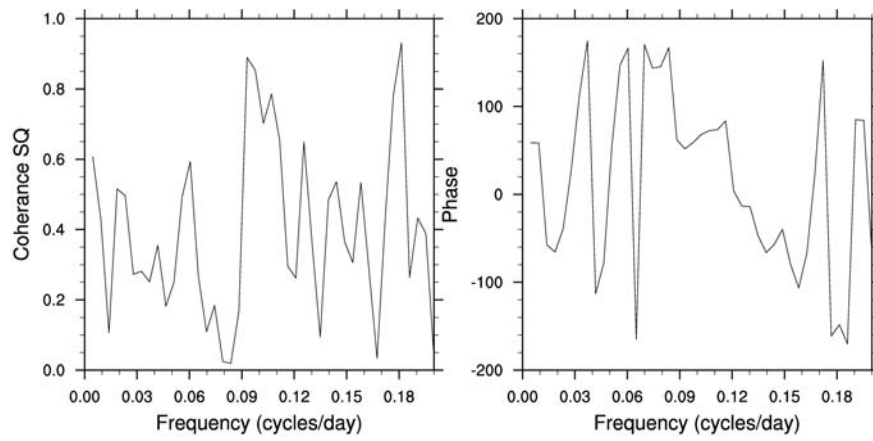


Figure 8: a) Coherence and b) phase angle between rainfall averaged over domain D1 ( $86^{\circ}$ -  $93^{\circ}$ E,  $22^{\circ}$ -  $27^{\circ}$ N) and salinity at RAMA buoy ( $15^{\circ}$ N,  $90^{\circ}$ E) for the time period 1<sup>st</sup> June to 31<sup>st</sup> **December** 2009.

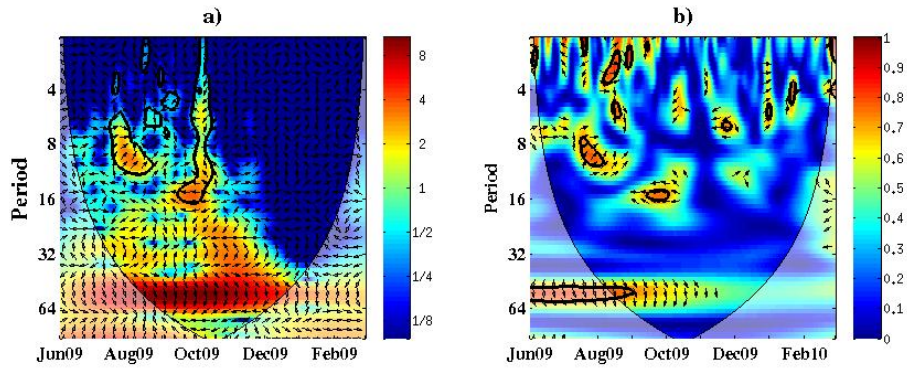


Figure 9: a) Wavelet co-spectrum and b) squared wavelet coherence between rainfall (averaged over D1) and salinity at RAMA buoy (top 35m averaged) for the period June-December 2009. Thick contour shows the area significant at 95% level and arrow indicates the phase angle between these two time series.



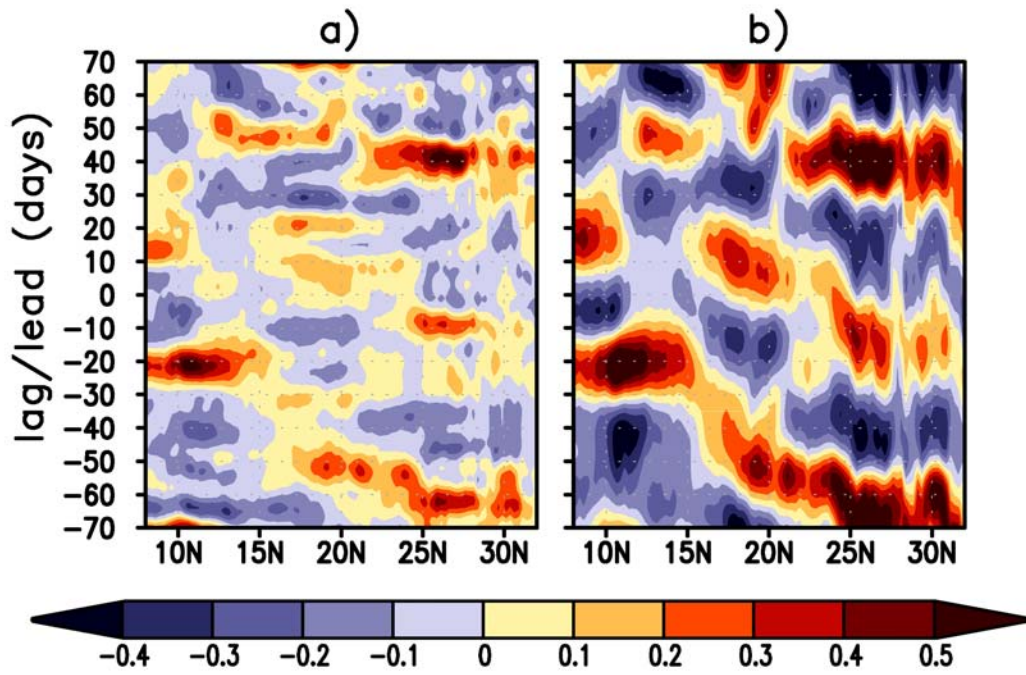


Figure 10: Lag-latitude section ( $88^{\circ}$ - $92^{\circ}$ E average) of regressed rainfall anomalies over D1 with top 35 m average salinity at RAMA buoy (1<sup>st</sup> June-31<sup>st</sup> December 2009). a) 10-100 days filtered anomalies, b) 30-60 days filtered anomalies.

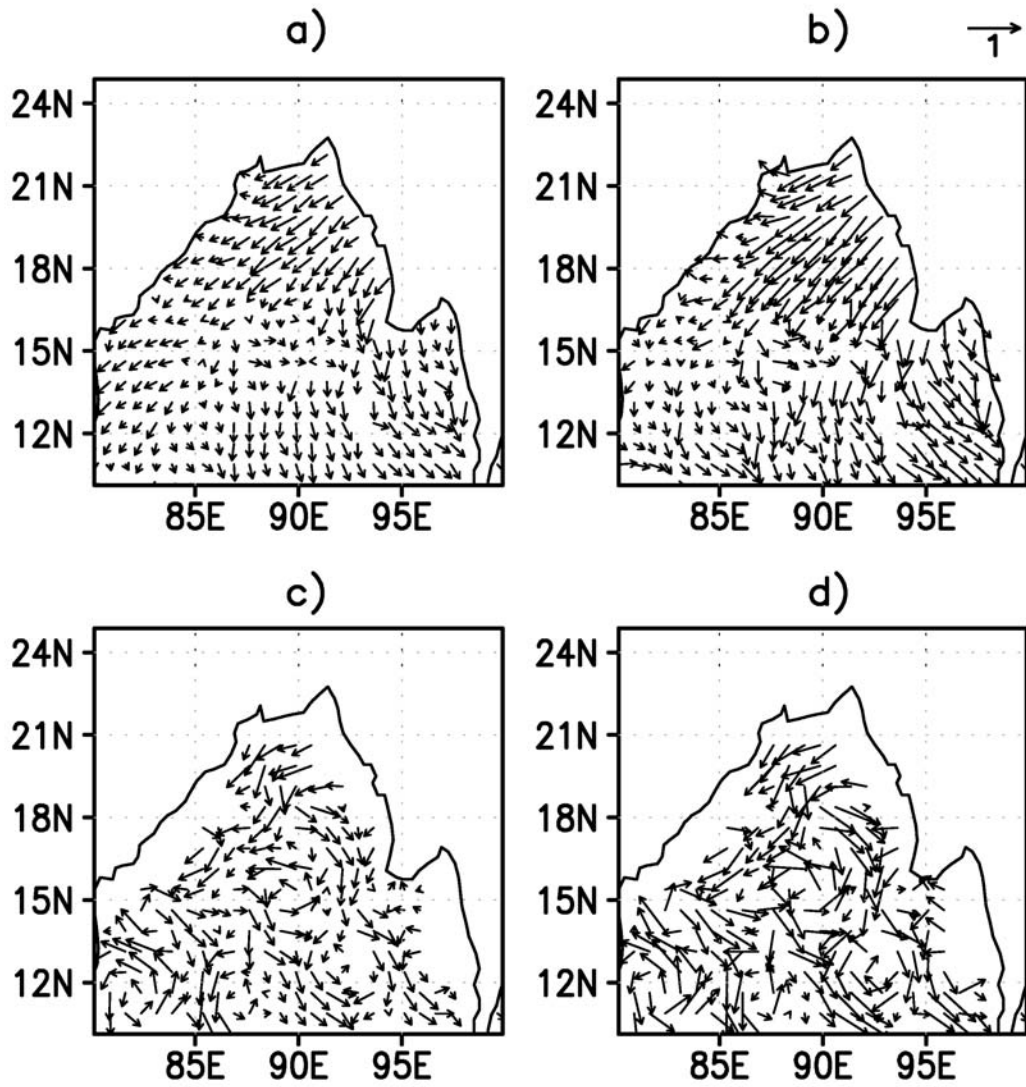


Figure 11: Regressed estimated current anomaly with top 35 m average salinity at RAMA buoy (1<sup>st</sup> June-31<sup>st</sup> October 2009). a) 10-100 days filtered Ekman current, b) 30-60 days filtered Ekman current, c) 10-100 days filtered total (Ekman + Geostrophy) current, d) 30-60 days filtered total current.